lncRNA C9orf139 can regulate the progression of esophageal squamous carcinoma by mediating the miR-661/HDAC11 axis

Xiaojie Yang
Fujian Medical University Union Hospital
Zhimin Shen
Fujian Medical University Union Hospital
Weiguang Zhang
Fujian Medical University Union Hospital
Yukang Lin
Fujian Medical University Union Hospital
Liming Li
Fujian Medical University Union Hospital
Tianci Chai
Fujian Medical University)Fujian Province University
Peipei Zhang
Fujian Medical University Union Hospital
Mingqiang Kang
Fujian Medical University Union Hospital
Jiangbo Lin (jiangbolin99@163.com)
Fujian Medical University Union Hospital

Research Article

Keywords: C9orf139, esophageal squamous carcinoma, miR-661, HDAC11, progression

Posted Date: March 10th, 2022

DOI: https://doi.org/10.21203/rs.3.rs-1418681/v1

Abstract

Background: Increasing evidence indicated that long non-coding RNAs (lncRNAs) play multiple functions in the development of cancer and function as indicator of diagnosis and prognosis. This study was to investigate the roles lncRNA C9ORF139 in the progression of esophageal squamous carcinoma (ESCC).

Methods: RT-qPCR analysis was employed to evaluate mRNA expressions. Western blot was performed to measure relevant protein level. Colony formation and CCK-8 assays were conducted to certify proliferative ability. Cell apoptosis and migration were measured using Annexin V-FITC and Transwell assay respectively. The underlying mechanism of lncRNA C9orf139 was surveyed by luciferase activity reporter assay and further verified using tumor xenograft in vivo. Protein-protein interaction network was built using STRING database.

Results: C9orf139 was highly expressed in ESCC and significantly suppressed cell proliferation, promoted apoptosis and inhibited migration and invasion. C9orf139 could negatively regulate miR-661 expression. While HDAC11 expression was negatively regulated by miR-661. C9orf139/miR-661/HDAC11 axis was further involved in regulating the expression of NF-κB signaling pathway. The association between the C9orf139 knockdown and the reduced tumor growth and size was observed in vivo study.

Conclusion: C9orf139 is highly expressed in ESCC, qualified to be used as a potential diagnostic and prognostic marker for pancreatic cancer. Its promotion of ESCC progression is achieved by mediating the miR-661/HDAC11 axis.

1 Introduction

Esophageal cancer (ESCA) is one of the most common cancers in the world, accounting for 11% of total cancer diagnoses each year[1, 2]. According to histopathological classification, esophageal carcinoma is mainly divided into esophageal squamous carcinoma (ESCC) and esophageal adenocarcinoma (EA). ESCC accounts for more than 90% of the confirmed cases of esophageal cancers in China[3, 4]. Although there are currently several treatments for ESCC that have been applied clinically[5, 6], there are still many limitations which have been brought about by technological development and lack of a more detailed understanding of the pathogenesis of ESCC, so the 5-year survival rate of it is only 22%-30%[7]. As is known to all, the early diagnosis and intervention of diseases are of great significance in the treatment of diseases. Therefore, it is of profound significance to explore the molecular mechanism of ESCC occurrence and development and, for the treatment of ESCC, to search for molecular targets by controlling the malignant development of ESCC and the improvement of prognosis and survival rate.

In the human genome, only 2% of expressed transcripts are protein-coding RNAs, while the rest are non-coding RNAs, of which long non-coding RNAs (lncRNAs) account for the largest proportion, about 80%[8, 9]. More and more studies have shown that changes in lncRNA expression profile are highly correlated with the progression of various cancers[10–12]. What is more interesting is that the interaction between lncRNAs and MicroRNAs has been mentioned in these studies. For example, lncRNA H19 could interact

with miR-138 and miR-200a to promote epithelial-mesenchymal transformation (EMT) in colorectal cancer[13]; LncRNA PAGBC could inhibit the functions of miR-133b and miR-511 and promote the occurrence of gallbladder tumor[14]. In general, lncRNAs combined microRNAs (miRNA /miRs) and act as miRNA sponges which would reduce their regulatory capacity[15]. As an important member of the lncRNA family, C9orf139 was found to be differentially expressed in various tumors, and expected to become a potential target for pancreatic cancer therapy[16]. And C9orf139 was highly expressed in pancreatic cancer and promoted pancreatic cancer cell growth by mediating the miR-663a /Sox12 axis[17]. In addition, bioinformatics analysis of patients with Pancreatic ductal adenocarcinoma (PDCA) indicated that C9orf139 was a promising prognostic indicator for PDCA[18].

MicroRNAs, as endogenous non-coding small RNAs, can inhibit gene expression by inhibiting mRNA translation and participate in post-transcriptional regulation of genes[19]. In recent years, the role of MicroRNAs in tumorigenesis and development has been extensively reported. Differences in the expression of miR-661 have been detected in different tumors and physiological functions which have been shown in diverse cells[20, 21]. However, the role of miR-661 in ESCC has not been reported in detail.

HDAC11, the newest member of the 11 human zinc-dependent HDACs, is also the smallest protein in this family and has the least characterized biological function. HDAC11 has been implicated in diverse immune functions[22], myoblast differentiation[23], metabolism, and obesity[24]. Its depletion has been reported to promote cell death and inhibit metabolic activity in HCT-116 colon, MCF7 breast, PC-3 prostate, and SK-OV-3 ovarian cancer cell lines[25]. In our study, we aimed to elucidate the molecular role of C9orfl39 in the tumorigenesis of ESCC and identify its potential interaction with miR-661/HDAC11 axis.

2 Material And Method

2.1 Cell lines, culture and transfection

Human esophageal cancer cell line TE-1, human esophageal cancer cell line ECA109, human embryonic kidney cell 293T were purchased from Beyotime, China. TE-1 cells were cultured in RPMI 1640(with 10% FBS,Gibco, Australia). ECA109, 293T were cultured in DMEM (with 10% FBS,Gibco, Australia). All cells were cultured in an incubator suitable for 37℃, 5%CO_2 and humidity.

shRNA-C9orf139, miR-661 mimics and anti-miR-661 inhibitor were synthesized by the company (50OD, purified by HPLC) and self-diluted for use. The pcDNA3.1-HDAC11 was derived from a subclone of the chemically synthesized CDS region of pcDNA3.1. Cells were collected, counted and seeded into 6-well plates the day before transfection. Cell transfection was performed by using lipofectamine 2000 (Invitrogen, Carlsbad, CA, USA), in accordance with the manufacturer's protocol. DMEM with 10% FBS was added to each well at 6 h following transfection.

2.2 RNA extraction and RT-qPCR

Collect total RNA by using kit reagents and mass of total RNA was evaluated by Nanodrop 2000 spectrophotometer(Thermo Scientific, America). Reverse transcription of 1.0 μg total RNA to cDNA and qPCR was performed by using the SYBR Green MasterMinds Kit Testing on the testing system platform(Biosystems 7500;ABI;America).The gene expression data was performed by 2 − ΔΔCt method to analysis the relative quantity.

2.3 Cell Counting Kit-8 (CCK-8) assay

Cells were inoculated 4000 cells/well into 96-well plates (100ul volume); 24h after cell inoculation, 100ul of fresh RPMI1640 medium (containing 2%FBS) was replaced. Lipofilter was about 0.6ul, 24.4ul was mixed with RPMI1640 medium (excluding FBS), and reached at room temperature for 5min. The prepared siRNA was about 50pmol (2ul)(or 0.25ug PCDNA3.1 plasmid containing the GENE CDS region) and mixed with 23ul RPMI1640 medium (excluding FBS). The prepared 2 tubes of solution were mixed, gently mixed, reached at room temperature for 20min, and then added into cells; After 6 hours of culture, 150ul of fresh RPMI1640 medium (containing 10%FBS) was replaced for further culture. After 72h foster, 10ul CCK8 reagent was added for further incubation for 1-4h. The absorbance was measured at 450nm.

2.4 Clone formation

A 6-well plate was taken, and the target cells of exponential growth period were inoculated :1000 cells/well. NC control group (or Ctrl group) and experimental group were set, and the number of cells could be adjusted appropriately according to experimental needs. 24h after cell inoculation, fresh RPMI1640 medium 1500ul (containing 2%FBS) was replaced. The lipofilter was about 5.0ul, mixed with 250ul RPMI1640 medium (containing 2%FBS), and reached at room temperature for 5min. The prepared siRNA was about 50pmol(2ul) or 0.25ug plasmid, and mixed with 250ul RMI1640 medium (containing 2%FBS). The prepared 2 tubes of solution were mixed, gently mixed, then left to reach at room temperature for 20 minutes before being added to cells. After 6h of culturing, 2000ul of fresh RMI1640 medium (containing 10%FBS) was replaced. After 7–10 days of continuous foster, the number of clones was observed under a microscope and photographed and counted.

2.5 Transwell assay

A 24-well Transwell plate was taken (pretreated with 0.2ml matrix glue for 1h), and the target cells (containing 5%FBS) in exponential growth period were inoculated in the upper chamber :10000 cells /250ul/ well, then NC control group and experimental group were set, with three multiple Wells/groups. 4h after cell inoculation, 2.4ul lipofilter was taken, 47.6ul was mixed in RPMI1640 medium (containing 5%FBS), and reached at room temperature for 5min.The prepared siRNA or microRNA was about 50pmol(2ul) or 0.25ug pcDNA3.1-HDAC11 plasmid, and mixed with 46ul RMI1640 culture base (containing 5%FBS). Mixed the prepared 2 tubes of solution, mixed gently, stood at room temperature for 20min, added into the cells and mixed gently again. After 6-12h culturing, 300ul of fresh RPMI1640 medium (containing 5%FBS) was replaced, and 500ul RPMI1640 medium (containing 20%FBS) was added into the lower chamber to continue culture. After 48 hours of culture, the upper chamber was removed and the cells attached to the upper surface of the upper chamber were gently scraped with

cotton swabs. The cells on the lower surface were treated and stained with crystal violet staining, and observed under a microscope then photographed.

2.6 Annexin V-FITC assay

Cells were inoculated during exponential growth period :100000 cells/well, NC control group and experimental group were set, and 3 multiple cells/group were set.24h after cell inoculation, 500ul of fresh RPMI1640 medium (containing 2%FBS) was replaced. 2.4ul lipofilter was taken, 47.6ul was mixed with RPMI1640 medium (containing 2%FBS), and stood at room temperature for 5min. The prepared siRNA was about 50pmol(2ul) or 0.25ug plasmid, and mixed with 46ul RPMI1640 medium (containing 2%FBS). Mix 2 tubes of solution, mix gently, let stand at room temperature for 20 minutes, then add into cells. After 6h culture, 500ul of fresh RPMI1640 medium (containing 10%FBS) was replaced. After 72h culture,300g,4, centrifugation for 5min. The cells were re-suspended by pre-cooled PBS and centrifuged at 300g,4, for 5min. Discard PBS and add 100ul 1*Binding buffer to resuscitate cells. Annexin V-FITC 5ul was added, mixed gently, dark, and reacted at room temperature for 10-15min. 400ul 1*Binding Buffer was added, mixed evenly and placed on ice for flow detection within 1h.

2.7 Dual luciferase activity detection

After 48h transfection, the cells were washed gently with PBS, followed by adding 200ul cell lysis solution to each well and incubating on ice for 5-10min to fully lysis the cells. According to the kit instructions (Shanghai YEASEN Biotechnology), luciferase substrate was prepared and kept on ice. 20ul cell lysate and 100ul firefly luciferase reaction solution was added into each well of the 96-well plate and then the plate was put into the plate tester to detect firefly luciferase activity. After the firefly luciferase activity was detected, 100ul of aquiferase reaction solution was added to each well and detect aquiferase activity.

2.8 Western blotting assay

After the experimental cells were washed twice with PBS solution, 100ul cell lysis buffer (containing 1% protease inhibitor 1%EDTA) was added, fully mixed, and reached at room temperature for 30sec. Centrifugation at 13000rpm for 5min. Took 20ul supernatant, added 5ul protein loading buffer, and mixed thoroughly. The samples were boiled in boiling water for 5min, and then some samples were taken. After electrophoresis, the membrane was transformed. Blocked PVDF membrane with blocking solution IKK antibody(ab32041) (1:500),IkB antibody(ab76429)(1:500), NFκB antibody(ab32360) (1 : 1,000), HDAC11 antibody (ab18973)(1 : 1,000), NCOR1 antibody(ab3482) (1 : 2,000),GAPDH antibody(ab8245)(1 : 3,000). Put them at room temperature for 1 h; added antibody diluted in blocking solution (goat anti rabbit IgG HRP (ab6721) (1: 3,000), and incubated them at 37℃ for 2 h and 4℃ overnight. Then, the membrane was washed and incubated with the goat anti rabbit IgG HRP antibody for 1h at 37℃. After washing the membrane, chemiluminescence imager was used for chemiluminescence.

2.9 Mouse Xenograft Assay

The effects of C9orf139 on tumorigenesis and growth in vivo were detected via mouse xenograft assay. We used twenty 5 to 6-week-old female NU-Foxn1nu nude mice (Vital River Laboratory Animal

Technology Co., Ltd., Beijing, China) for the mouse xenograft assay. A total of 3×10^6 TE-1-NC cells or C9orf139-knockdown stable TE-1 cells were used to inject into the right or left oxter of female NU-Foxn1nu nude mice, respectively. Tumor size and weight were determined with calipers and balanced twice a week. The mice were executed and the tumors were removed after 53 days. The formula V = (W 2×L)/2 was used to calculate the tumor volume. V is the tumor volume, W is the tumor width, and L is the tumor length. Tumor size was presented as mean ± standard deviation (SD).

2.10 Protein-protein interactionnetwork

The PPI interaction networks between the DEGs were constructed by Search Tool for the Retrieval of Interacting Genes (STRING) database (http://string-db.org/)[26]. Firstly, the DEGs were typed into the database. Then, high-resolution bitmaps were displayed and downloaded from the webpage. Only these interactors with combined confidence score > = 0.4 were shown in the bitmap.

2.11 Statistical analysis

All experiments were repeated at least 3 times during the study period. Statistical analysis was performed using GraphPad Prism 8 software (GraphPad Software, Inc., La Jolla, CA, USA). All data are expressed as mean ± standard deviation (SD) unless otherwise stated. The main statistical methods were tested and one-way ANOVA ($p < 0.05$ was considered significant in STATISTIC).

3 Results

3.1 Interactions of C9orf139/ miR-661 /HDAC11

First of all, we detected the expression of C9orf139 in normal esophageal epithelial cells and esophageal carcinoma cells (ECA10, TE-1 and TE-12). qPCR results showed that the expression of C9orf139 was significantly increased in esophageal cancer cells, especially in ECA109 cell line (Fig. 1A). In addition, we detected the cytoplasmic distribution of C9orf139 in TE-1 and ECA109 cell lines, and found that the distribution of C9orf139 in the cytoplasm of the two cancer cells was much higher than that in the nucleus (Fig. 1B, C). Subsequently, we constructed shrNA-C9orf139 vector and transfected TE-1 and ECA109 cell lines. ShC9orf139-#1 fragment with better knockdown effect (over 70%) was selected for subsequent experiments (Fig. 1D). It was interesting to note that miR-661 was significantly elevated after down-regulation of C9orf139 gene expression (Fig. 1E). Therefore, miR-661 mimics and anti-miR-661 inhibitor molecules were constructed in an attempt to search for downstream molecules of miR-661 inhibitor. After mir-661 expression was increased or decreased, HDAC11 gene expression was decreased or increased, and there would be a negative correlation between the two (Fig. 1F-I).

3.2 C9orf139/ miR-661 /HDAC11 regulated cell proliferation

After determining the intermolecular interaction of C9orf139/ miR-661 /HDAC11, we first explored the function of this signal axis. As shown in Fig. 2A, the proliferation ability of TE-1 was significantly reduced after the down-regulation of C9orf139 expression, which was consistent in ECA109 cells (Fig. 2B). The proliferation ability of cells was partially restored, and the inhibition caused by the down-regulation of C9orf139 was relieved to a certain extent, after the inhibition of miR-661 expression. (Fig. 2C, D). Overexpression of HDAC11 led to the same results (Fig. 2E, F). Similarly, after the expression of C9orf139 was knocked down, the clonogenesis ability of the cells was decreased (Fig. 2G). Inhibition of miR-661 or overexpression of HDAC11 resulted in the release of inhibition and partial recovery of clonogenesis (Fig. 2H, I).

3.3 C9orf139/ Mir-661 /HDAC11 and tumor invasion

In previous experiments, we found that the C9orf139/ miR-661 /HDAC11 signaling axis regulated the proliferation of esophageal cancer cells. Further, we analyzed the relationship between this signal axis and tumor invasion ability. We pre-inoculated 0.2ml Matrigel (mainly composed of laminin and collagen type Ⅳ) at the bottom of the chamber, and inserted the cells according to the number of 1×10^5 cells. After grouping, the cells were cultured for 48h and observed by crystal violet staining. The results showed that the invasion ability of BOTH TE-1 and ECA109 cells was significantly reduced after the expression of C9orf139 was down-regulated (Fig. 3A). Reduced miR-661 expression or the up-regulation of HDAC11 both, to a large extent, restored the invasion ability of tumor cells (Fig. 3B, C).

3.4 C9orf139 knockdown induced apoptosis

Similarly, we used the previous grouping model to analyze the effect of C9orf139 on the apoptosis of esophageal cancer cells. Similar to the previous results, knockdown C9orf139 remarkably increased the apoptosis rate of TE-1 and ECA109 cells (Fig. 4A, B). When miR-661 was inhibited, the apoptosis rate of tumor cells was dramatically reduced (Fig. 4C, D), and the results were consistent with the one after HDAC11 was upregulated (Fig. 4E, F).

3.5 Signal transduction mechanism between C9orf139/ miR-661 /HDAC11

Our study found that the C9orf139/ miR-661 /HDAC11 signal axis was closely related to the proliferation, invasion and apoptosis of esophageal cancer cells. Therefore, the signal transduction mechanism between the signal axis and the molecular pathways that induced cell proliferation, apoptosis and other related changes became the key which need to be urgently solved. First, we validated the molecular interactions among C9orf139, miR-661 and HDAC11 by using a dual-luciferase system. As shown in Fig. 5A and B, miR-661 mimics significantly reduced luciferase expression driven by C9orf139, while luciferase expression recovered after miR-661 mutation. Similarly, miR-661 mimics significantly lessened luciferase expression driven by HDAC11-3-UTR, and luciferase expression recovered after site mutation (Fig. 5C,D). In addition, mir-661 mimics inhibited HDAC11-3-UTR-driven Luciferase expression in TE-1 cells after co-transfection with C9orf139 (Fig. 5E).

Extensive studies have shown that NFκB pathway is involved in the regulation of immune responses in the body, and is closely related with cell proliferation and migration. Therefore, we first verified the possible relationship between C9orf139 and NFκB signaling pathway. After C9orf139 gene was knocked down, NF-κB and IKK expressions were decreased, and IκB expression was increased. The expression of HDAC11 also decreased correspondingly (Fig. 5F, G). The interaction between NCOR1 and HDAC11 was found by String database analysis (Fig. 5H). WB assay confirmed that decreased expression of C9orf139 gene resulted in decreasing expression of HDAC11 but increasing expression of NCOR1(Fig. 5F, G). Inhibition of miR-661 expression could restore some of the effects of C9orf139 knockdown (Fig. 5F, G).

3.6 Tumor growth inhibition induced by knockdown of C9orf139 gene in vitro

We constructed a mouse xenograft model through subcutaneous injection to further verify the effect of C9orf139 knockout on tumor growth in vivo. TE-1 cells were transfected with NC and shC9orf139-#1 respectively, and then xenografted with mouse xenograft after cell expansion. It was found that compared with the control group, tumor growth of mice inoculated with shC9orf139-#1-TE-1 cells was slower, tumor volume was significantly reduced, and tumor volume was lighter than that of the control group (Fig. 5I-K).

4 Discussion

The Esophageal cancer (EC) ranks seventh in the incidence of cancer worldwide and sixth in cancer-specific mortality[27]. ESCC accounts for about 90% of all EC histological subtypes[28]. Despite recent advances in minimally invasive techniques, optimization of chemoradiotherapy protocols, and molecular targeted therapy innovations, ESCC treatment and prognosis 5-year survival remain low[29, 30]. Therefore, it is crucial for the diagnosis and treatment of ESCC to search for molecular targets related to the treatment of ESCC and to further study a series of prognostic indicators that can accurately predict the outcome of surgery, which is the key of the current ESCC research.

In recent years, different kinds of non-coding RNAs have become the focus of research in various fields. In recent years, studies on microRNAs have focused on tumor drug resistance and autophagy[31, 32], while lncRNAs are mainly focused on their differential expression and gene regulation functions in different types of cancer[11, 33]. More and more studies have found that lncRNAs can act as molecular sponges and interact with microRNAs to regulate gene expression. C9orf139, as an important member of the lncRNA family, has been reported to be associated with the growth of pancreatic cancer cells[17] and the prognostic indicators of PDCA patients[18]. Our study confirmed that C9orf139 can regulate downstream HDAC11 expression through interaction with miR-661, and affect the proliferation, invasion and apoptosis of esophageal cancer tumor cells from both in vitro and in vivo. The discovery of C9orf139/ miR-661 /HDAC11 signaling axis further complicates the role of C9orf139 in the growth and migration of esophageal cancer cells, and provides a potential target for the treatment of esophageal cancer.

Previous studies have focused on the regulatory role of immune cells in the NF-KB signaling pathway, and recent studies have found that the NF-KB signaling pathway is closely related to tumor proliferation and migration[34–36]. Dai D et al. demonstrated that PELI1 regulated the sensitivity of tumor cells to radiotherapy by regulating ir-induced atypical NF-κB expression[37]. In our study, downregulation of C9orf139 resulted in decreasing molecular expression of NF-κB,IKK, and the target gene HDAC11, as well as enhanced expression of IκB, which was restored after inhibition of miR-661. Consistent with previous findings, this study showed that C9orf139/ miR-661 /HDAC11 signaling axis was involved in the regulation of NF-KB signaling pathway, and was closely related to the proliferation, invasion and apoptosis of esophageal cancer cells. Our study promoted the clarification of the molecular function of C9orf139 and the study of potential therapeutic targets for ESCC, and provided a new candidate indicator for the prognostic detection of ESCC.

Declarations

Author Contributions: XY and ZS contributed equally to this study. MK and JL conceived and corresponded to this study together. XY and ZS performed the experiments, analyzed the data and drafted the manuscript. WZ, YL, LL contributed to data analysis. TC and PZ discussed the results. MK and JL revised the manuscript.

Funding: This work was supported by Fujian provincial health technology project (2020CX01010103), Fujian Provincial Natural Science Foundation General Project (2021J01745)Fujian Provincial Natural Science Foundation General Project (2020J01997), Young and Middle-aged Teacher Education Research Project of Fujian Education Department (JAT190194) and Sailing Fund General Project of Fujian Medical University (2019QH1023).

Data availability: The data used to support the findings of this study are available from the corresponding author upon request.

Ethics approval and consent to participate: The experimental protocols were approved by the Ethics Committee of the Fujian Medical University Union Hospital (Reference 20210201). This paper has not been published elsewhere in whole or in part. All authors have read and approved the content, and agree to submit it for consideration for publication in your journal. There are no ethical/legal conflicts involved in the article

Competing interests: The authors have declared no conflicts of interest in this work

References

1. Kroep S, Lansdorp-Vogelaar I, Rubenstein JH, de Koning HJ, Meester R, Inadomi JM, et al. An Accurate Cancer Incidence in Barrett's Esophagus: A Best Estimate Using Published Data and Modeling. Gastroenterology. 2015;149:577–85. e4; quiz e14-5.

2. Xu J, Kang D, Xu M, Zhuo S, Zhu X, Chen J. Multiphoton microscopic imaging of esophagus during the early phase of tumor progression. Scanning. 2013;35:387–91.
3. Chen W, Zheng R, Baade PD, Zhang S, Zeng H, Bray F, et al. Cancer statistics in China, 2015. CA Cancer J Clin. 2016;66:115–32.
4. Liang H, Fan JH, Qiao YL. Epidemiology, etiology, and prevention of esophageal squamous cell carcinoma in China. Cancer Biol Med. 2017;14:33–41.
5. Shafaee A, Dastyar DZ, Islamian JP, Hatamian M. Inhibition of tumor energy pathways for targeted esophagus cancer therapy. Metabolism. 2015;64:1193–8.
6. Khat'kov IE, Izrailov RE, Domrachev SA, Kononets PV, Vasnev OS, Koshkin MA. [Thoracolaparoscopic simultaneous operations on esophagus]. Khirurgiia (Mosk). 2014;45–51.
7. Allemani C, Matsuda T, Di Carlo V, Harewood R, Matz M, Niksic M, et al. Global surveillance of trends in cancer survival 2000-14 (CONCORD-3): analysis of individual records for 37 513 025 patients diagnosed with one of 18 cancers from 322 population-based registries in 71 countries. Lancet. 2018;391:1023–75.
8. Kopp FMendell JT. Functional Classification and Experimental Dissection of Long Noncoding RNAs. Cell. 2018;172:393–407.
9. Noh JH, Kim KM, McClusky WG, Abdelmohsen K, Gorospe M. Cytoplasmic functions of long noncoding RNAs. Wiley Interdiscip Rev RNA. 2018;9:e1471.
10. Chen R, Li WX, Sun Y, Duan Y, Li Q, Zhang AX, et al. Comprehensive Analysis of lncRNA and mRNA Expression Profiles in Lung Cancer. Clin Lab. 2017;63:313–20.
11. Jiang B, Yang B, Wang Q, Zheng X, Guo Y, Lu W. lncRNA PVT1 promotes hepatitis B viruspositive liver cancer progression by disturbing histone methylation on the cMyc promoter. Oncol Rep. 2020;43:718–26.
12. Jin L, Fu H, Quan J, Pan X, He T, Hu J, et al. Overexpression of long non-coding RNA differentiation antagonizing non-protein coding RNA inhibits the proliferation, migration and invasion and promotes apoptosis of renal cell carcinoma. Mol Med Rep. 2017;16:4463–8.
13. Liang WC, Fu WM, Wong CW, Wang Y, Wang WM, Hu GX, et al. The lncRNA H19 promotes epithelial to mesenchymal transition by functioning as miRNA sponges in colorectal cancer. Oncotarget. 2015;6:22513–25.
14. Wu XS, Wang F, Li HF, Hu YP, Jiang L, Zhang F, et al. LncRNA-PAGBC acts as a microRNA sponge and promotes gallbladder tumorigenesis. EMBO Rep. 2017;18:1837–53.
15. Paraskevopoulou MDHatzigeorgiou AG. Analyzing MiRNA-LncRNA Interactions. Methods Mol Biol. 2016;1402:271–86.
16. Song J, Xu Q, Zhang H, Yin X, Zhu C, Zhao K, et al. Five key lncRNAs considered as prognostic targets for predicting pancreatic ductal adenocarcinoma. J Cell Biochem. 2018;119:4559–69.
17. Chen S, Ju G, Gu J, Shi M, Wang Y, Wu X, et al. Competing endogenous RNA network for esophageal cancer progression. Ann Transl Med. 2021;9:1473.

18. Ge JN, Yan D, Ge CL, Wei MJ. LncRNA C9orf139 can regulate the growth of pancreatic cancer by mediating the miR-663a/Sox12 axis. World J Gastrointest Oncol. 2020;12:1272–87.
19. Zeng Y, Yi R, Cullen BR. MicroRNAs and small interfering RNAs can inhibit mRNA expression by similar mechanisms. Proc Natl Acad Sci U S A. 2003;100:9779–84.
20. Zhu T, Yuan J, Wang Y, Gong C, Xie Y, Li H. MiR-661 contributed to cell proliferation of human ovarian cancer cells by repressing INPP5J expression. Biomed Pharmacother. 2015;75:123–8.
21. Li Z, Liu YH, Diao HY, Ma J, Yao YL. MiR-661 inhibits glioma cell proliferation, migration and invasion by targeting hTERT. Biochem Biophys Res Commun. 2015;468:870–6.
22. Huang J, Wang L, Dahiya S, Beier UH, Han R, Samanta A, et al. Histone/protein deacetylase 11 targeting promotes Foxp3 + Treg function. Sci Rep. 2017;7:8626.
23. Villagra A, Cheng F, Wang HW, Suarez I, Glozak M, Maurin M, et al. The histone deacetylase HDAC11 regulates the expression of interleukin 10 and immune tolerance. Nat Immunol. 2009;10:92–100.
24. Bhaskara S. Histone deacetylase 11 as a key regulator of metabolism and obesity. EBioMedicine. 2018;35:27–8.
25. Deubzer HE, Schier MC, Oehme I, Lodrini M, Haendler B, Sommer A, et al. HDAC11 is a novel drug target in carcinomas. Int J Cancer. 2013;132:2200–8.
26. Szklarczyk D, Franceschini A, Kuhn M, Simonovic M, Roth A, Minguez P, et al. The STRING database in 2011: functional interaction networks of proteins, globally integrated and scored. Nucleic Acids Res. 2011;39:D561-8.
27. Sung H, Ferlay J, Siegel RL, Laversanne M, Soerjomataram I, Jemal A, et al. Global Cancer Statistics 2020: GLOBOCAN Estimates of Incidence and Mortality Worldwide for 36 Cancers in 185 Countries. CA Cancer J Clin. 2021;71:209–49.
28. Collaborators GBDOC. The global, regional, and national burden of oesophageal cancer and its attributable risk factors in 195 countries and territories, 1990–2017: a systematic analysis for the Global Burden of Disease Study 2017. Lancet Gastroenterol Hepatol. 2020;5:582–97.
29. Jemal A, Siegel R, Ward E, Murray T, Xu J, Thun MJ. Cancer statistics, 2007. CA Cancer J Clin. 2007;57:43–66.
30. Wang Q, Peng L, Han Y, Li T, Dai W, Wang Y, et al. Preoperative Serum Sodium Level as a Prognostic and Predictive Biomarker for Adjuvant Therapy in Esophageal Cancer. Front Oncol. 2020;10:555714.
31. Lin YH. MicroRNA Networks Modulate Oxidative Stress in Cancer. Int J Mol Sci. 2019;20.
32. Rupaimoole RSlack FJ. MicroRNA therapeutics: towards a new era for the management of cancer and other diseases. Nat Rev Drug Discov. 2017;16:203–22.
33. Jathar S, Kumar V, Srivastava J, Tripathi V. Technological Developments in lncRNA Biology. Adv Exp Med Biol. 2017;1008:283–323.
34. Lee DFHung MC. Advances in targeting IKK and IKK-related kinases for cancer therapy. Clin Cancer Res. 2008;14:5656–62.
35. Napetschnig JWu H. Molecular basis of NF-kappaB signaling. Annu Rev Biophys. 2013;42:443–68.

36. Sun SC, Chang JH, Jin J. Regulation of nuclear factor-kappaB in autoimmunity. Trends Immunol. 2013;34:282–9.
37. Dai D, Zhou H, Yin L, Ye F, Yuan X, You T, et al. PELI1 promotes radiotherapy sensitivity by inhibiting noncanonical NF-kappaB in esophageal squamous cancer. Mol Oncol. 2021.

Figures

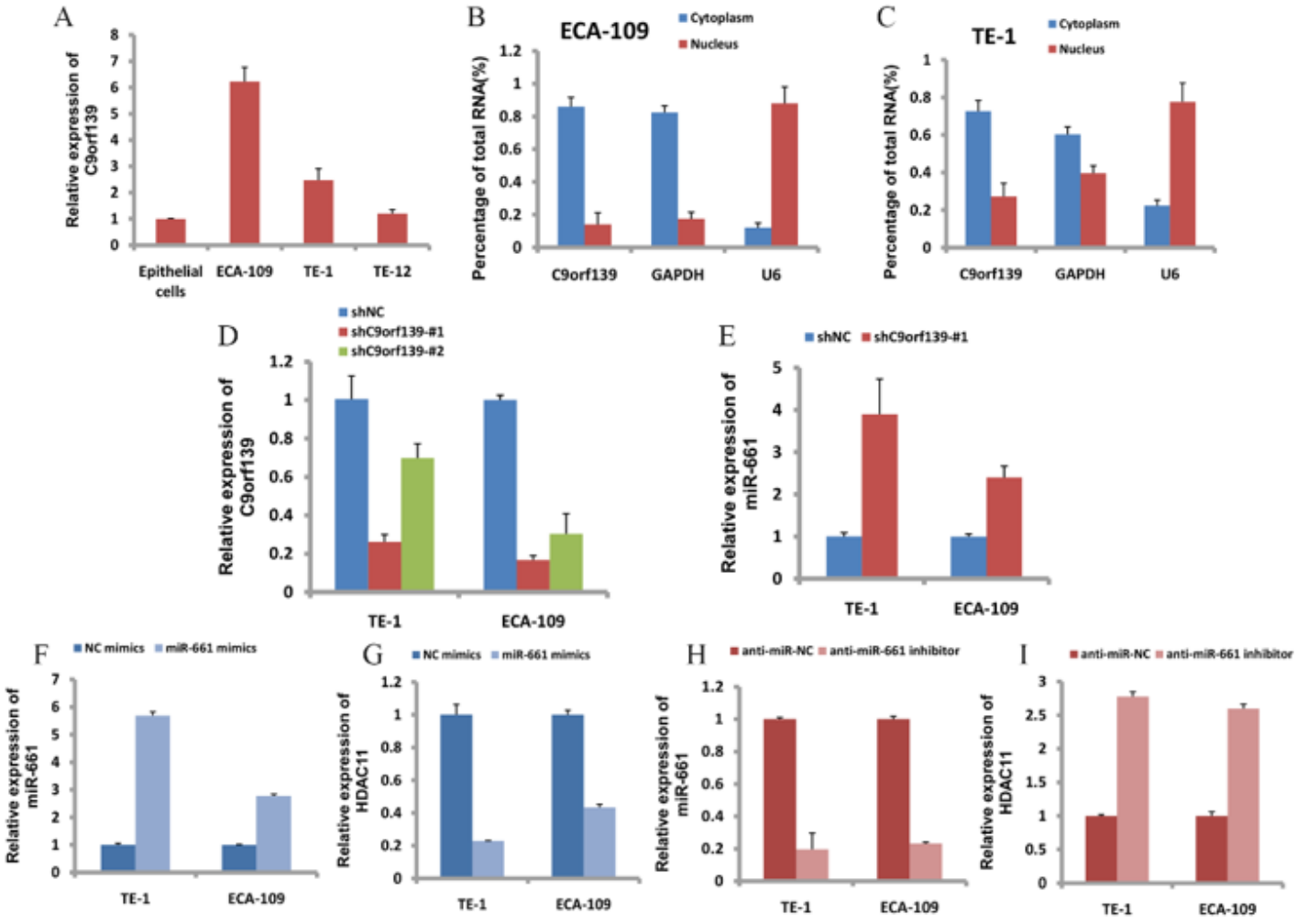

Figure 1

Interactions of C9orf139/ miR-661 /HDAC11. (A) qPCR assay was used to detect the expression of C9orf139 in normal esophageal cells which called ECA109,TE-1 and TE-12.(B-C) Cell localization of C9orf139 in TE-1 and ECA109 cells.(D) The shC9orf139-#1 and shC9orf139-#2 infection efficiency of TE-1 cells and ECA109 cells were analyzed by qPCR，compared with shNC group，C9orf139 protein levels were down-regulated in both interference groups.(E) Effect of C9orf139 knockdown on miR-66 in TE-1 and ECA109 cells.(F-G) Effect of miR-661 mimics on HDAC11 gene expression.(H-I) Effect of anti-miR-661 inhibitor on HDAC11 gene expression. Data were presented as mean ± SD. *(*P < 0.05,**P < 0.01,***P < 0.001.)*

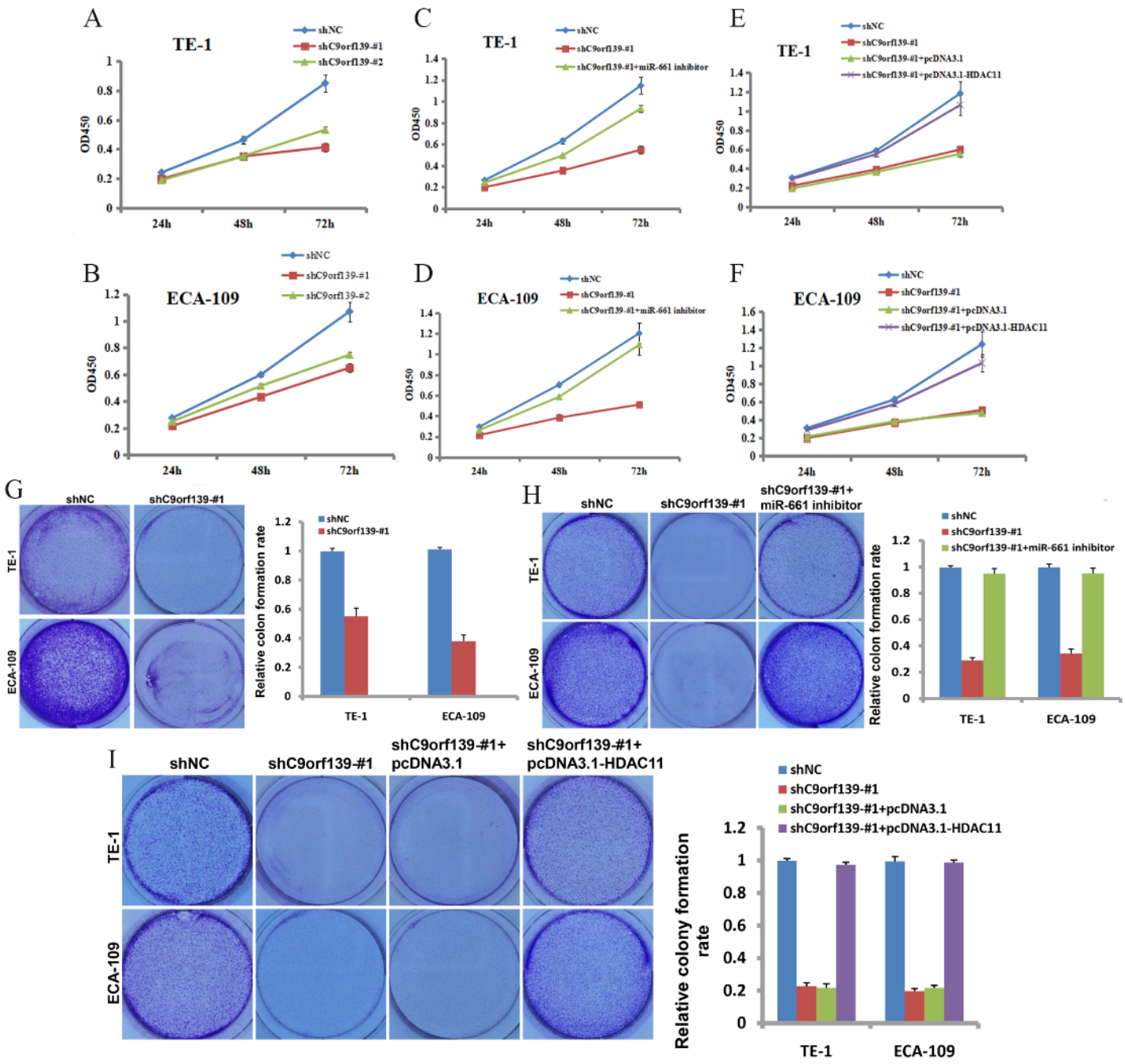

Figure 2

C9orf139/ miR-661 /HDAC11 regulated cell proliferation and clonal formation. (A)Proliferation of TE-1 cells after transfection with C9orf139 knockdown plasmid.(B)Proliferation of ECA109 cells after transfection with C9orf139 knockdown plasmid.(C-D)Cells proliferation were detected by CCK8,and growth inhibition induced by shC9orf139-#1 was removed after transfection with miR-661 inhibitor.(E-F) Cells proliferation were detected by CCK8, and growth inhibition induced by shC9orf139-#1 was relieved after overexpression of HDAC11.(G-H)Same as the above experimental groups, clone formation ability was detected and counted.(Data were presented as mean ± SD. *(*P < 0.05,**P < 0.01,***P < 0.001.)*

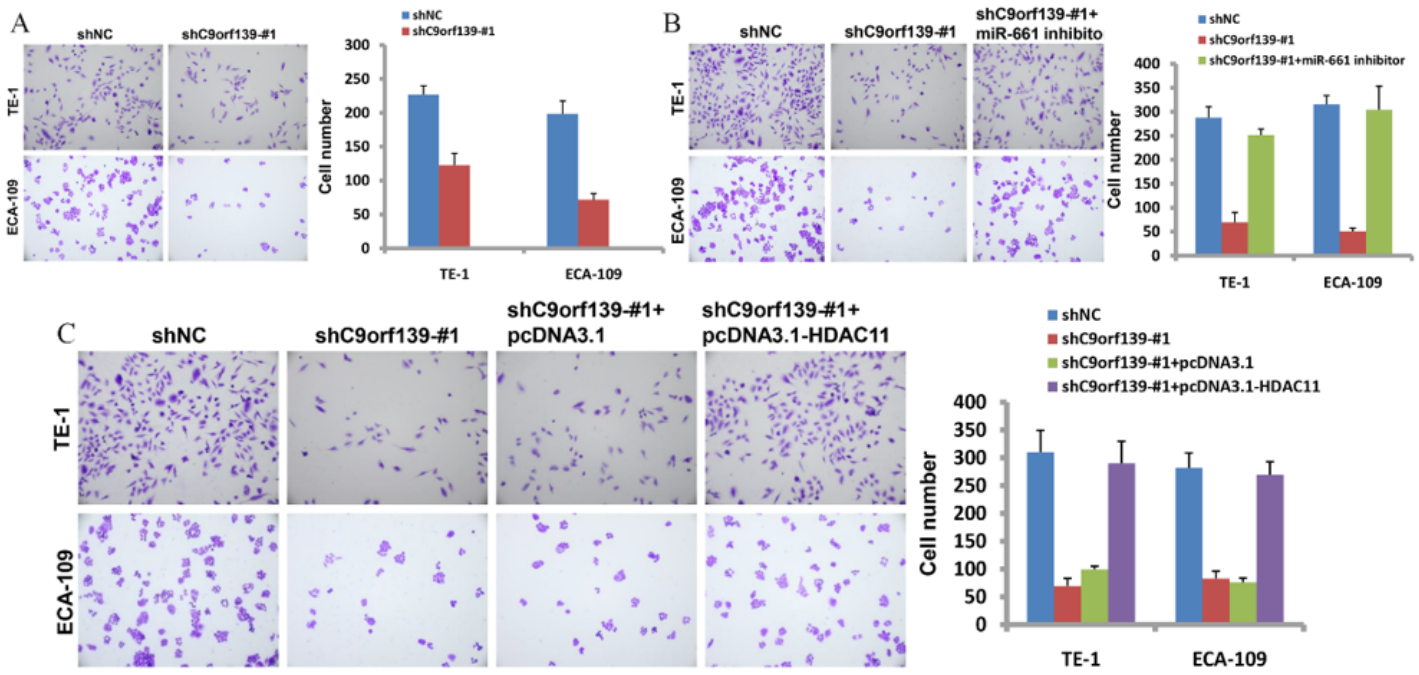

Figure 3

C9orf139/ miR-661 /HDAC11 regulated ESCC cell invasion. (A) Tumor invasion test: The invasion of tumor cells was weakened by knocking down the expression of C9orf139 gene.(B) Tumor invasion test: Compared with shNC, the tumor invasion ability of shC9orf139-#1 group was reduced, and the invasion ability was recovered after co-transfection with Mir-661 inhibitor.(C) Tumor invasion assay: Compared with shNC, the tumor invasion ability of shC9orf139-#1 group decreased, and the invasion ability was restored after co-transfection with pcDNA3.1-HDAC11.(Data were presented as mean ± SD. *(*P < 0.05,**P < 0.01,***P < 0.001.)*

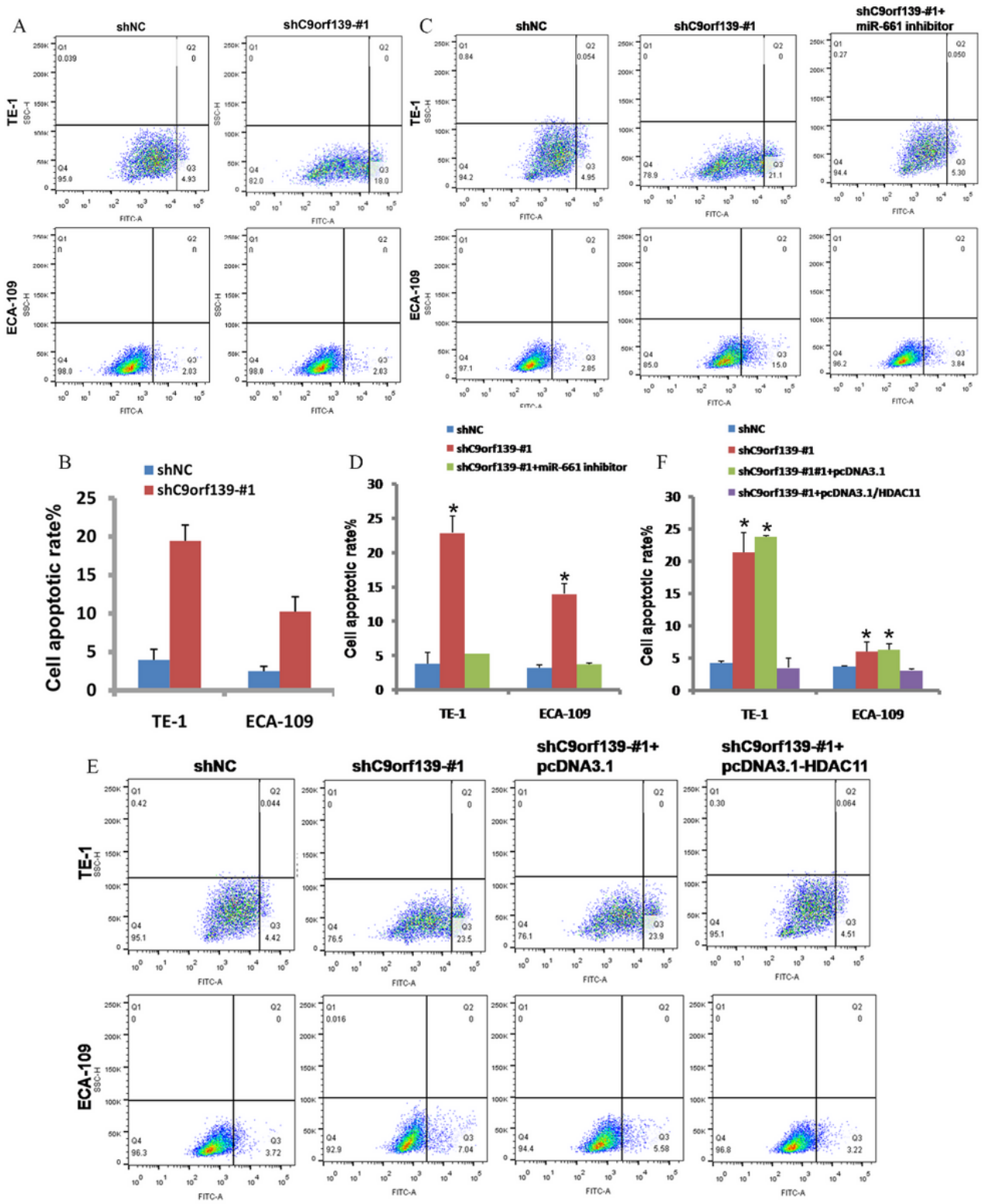

Figure 4

C9orf139/ miR-661 /HDAC11 regulated tumor cell apoptosis (A-C) Apoptosis was detected by Annexin V-FITC assay. A: C9orf139 knockdown resulted in increasing apoptosis: Knockdown of C9orf139 could significantly enhance the apoptosis of esophageal cancer cells, and the apoptosis rate of cancer cells was conspicuously reduced when miR-661 was inhibited. C: Knockdown of C9orf139 induced apoptosis

of esophageal cancer cells, which was inhibited by overexpression of HDAC11. (Data were presented as mean ± SD. *(*P < 0.05,**P < 0.01,***P < 0.001.)*

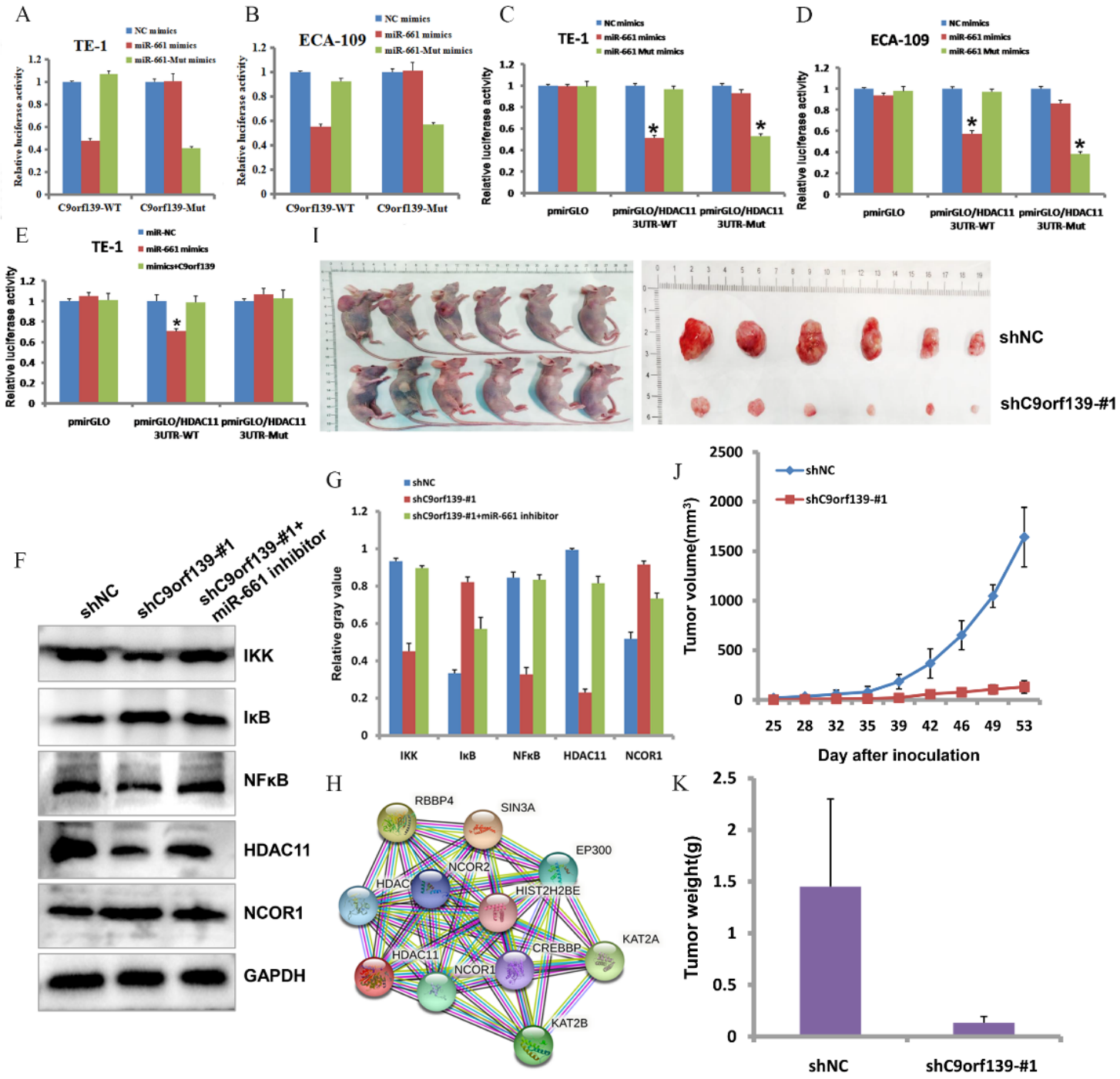

Figure 5

Signal transduction mechanism between C9orf139/ miR-661 /HDAC11 and mouse xenograft model. (A-E) Double luciferase assay. A-B: miR-661 mimics significantly reduced the expression of Luciferase driven by C9orf139, while luciferase expression recovered after site mutation. C-D: miR-661 mimics significantly lessened luciferase expression driven by HDAC11-3-UTR, while luciferase expression recovered after site

mutation. E:In TE-1 cells, miR-661 mimics significantly reduced luciferase expression driven by HDAC11-3-UTR, but increased luciferase expression after co-transfection with C9orf139.(F) The regulation of NFκB signaling pathway by C9orf139/ miR-661 /HDAC11 was detected by WB.(G) Gray analysis of F. (H) String database predicted HDAC11 key interacting proteins.(I)The mice xenograft models and tumors.(J) The volumetric of tumors was measured after removing the tumors from the mice xenograft models.(K)Tumor weight of xenograft model mice was measured. Data were presented as mean ± SD. *(*P < 0.05,**P < 0.01,***P < 0.001.)*